Molecular Crystals and Liquid Crystals
Publication details, including instructions for authors and subscription information:
http://www.tandfonline.com/loi/gmcl16

Contrasting Solid-State Structures for Two Nematogenic Benzylideneanilines. Crystal Structures of p [(p'-Ethoxybenzylidene)amino] -benzonitrile and p- [(p'-Methoxybenzylidene)amino] -phenyl Acetate

R. F. Bryan [a] & P. G. Forcier [a]
[a] Chemistry Department, University of Virginia, Charlottesville, Virginia, 22901, USA
Version of record first published: 20 Apr 2011.

Mol. Cryst. Liq. Cryst., 1980, Vol. 60, pp. 133–152
0026-8941/80/6001–0133$04.50/0

Printed in the U.S.A.

Contrasting Solid-State Structures for Two Nematogenic Benzylideneanilines. Crystal Structures of *p*-[(*p'*-Ethoxybenzylidene)amino]-benzonitrile and *p*-[(*p'*-Methoxybenzylidene)amino]-phenyl Acetate

R. F. BRYAN and P. G. FORCIER

Chemistry Department, University of Virginia, Charlottesville, Virginia 22901, USA

(*Received August 3, 1979; in final form November 8, 1979*)

The crystal structures of two nematogens, *p*-[(*p'*-ethoxybenzylidene)amino]benzonitrile (EOBABN) and *p*-[(*p'*-methoxybenzylidene)amino]phenyl acetate (MOBAPA), have been determined as part of a study of the relations between crystal structure and liquid crystallinity. In EOBABN the molecules are arranged in a head-to-tail fashion in rows parallel to the crystal *b*-axis, with which the molecular long axes make angles of $\pm 12.5°$. This structure is of a common type for nematogens, and could transform to the nematic state by means of a simple *displacive* transition where the molecules acquire three translational, but at most one rotational, degrees of freedom. In MOBAPA the crystal structure is made up of bimolecular sheets in which the long molecular axes lie in parallel planes normal to the sheet surface, but are inclined to the surface at $\pm 19°$. The director axes of successive sheets lie in the sheet planes, but are mutually perpendicular from one sheet to the next. To proceed to a classical nematic phase from this solid-state arrangement would require a *reconstitutive* transition involving an initial rotation of the molecules about an axis other than the long axis. A reversible solid-solid transition is observed for this material about 3° below the solid-nematic transition, so that it is not certain at which transition such motions occur, if at all.

Crystals of EOBABN have space group $P2_1/c$, with $a = 7.817(2)$, $b = 16.208(5)$, $c = 11.490(4)$ Å, $\beta = 112.76(5)°$, and $Z = 4$. Crystals of MOBAPA have space group $Pna2_1$, with $a = 19.833(5)$, $b = 5.858(2)$, $c = 12.210(4)$ Å, and $Z = 4$. Each structure was solved by direct methods. Least-squares refinement gave $R = 0.040$ for 1362 independent significant reflections in EOBABN, and $R = 0.054$ for 962 reflections in MOBAPA.

INTRODUCTION

It is a generally accepted structural feature of nematic phases that the highly anisotropic molecules from which they are constituted are arranged locally so that their long axes are parallel, or nearly so, and that there is no local ordering of the molecular centers of mass.[1] This local parallelism is also believed to extend in three dimensions over distances which are large compared to molecular dimensions so that a single order parameter serves to define the orientational order of molecules in the phase.[2]

Two types of transition from the solid state to the nematic mesophase may be conceived. The first type, which we may designate as a *displacive* transition,[3] involves comparatively limited displacements of the molecules from the positions which they occupy with respect to their nearest neighbors in the crystal. Expressed in terms of molecular degrees of freedom, the molecules acquire three translational degrees of freedom but rotation is restricted to, at most, motion about the long molecular axis. In the second type of transition, designated as *reconstitutive*, the molecular arrangement in the solid must alter in a more pronounced fashion to achieve the presumed mesophase arrangement. Such transitions will normally call for rotations of molecules about axes other than the long axis, and may also be accompanied by changes in molecular conformation.

Surprisingly few identifiable examples of crystal structures associated with reconstitutive transitions have been reported. With but a single exception,[4] the crystal structures of all nematogens thus far reported are of a kind where the transition to the mesophase may be assumed to be of the displacive type.[5] This dominant structural category already has the long axes of the molecules arranged in the parallel, or nearly parallel, fashion assumed to characterize the mesophase organization. We report here the crystal structures of two nematogenic Schiff's bases, for one of which a reconstitutive transition would be required if it is assumed that the mesophase to which it gives rise is of the classical type.

The crystal structure of the first compound,

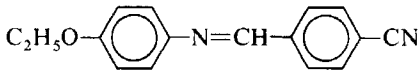

p-[(*p*'-ethoxybenzylidene)amino]benzonitrile (EOBABN), which yields a nematic phase between 105 and 124.5°,[6] has a molecular arrangement in which the molecular long axes do not deviate by more than 12.5° from a common direction.

The second compound, *p*-[(*p*'-methoxybenzylidene)amino]phenyl

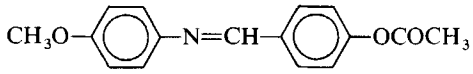

acetate (MOBAPA), undergoes a reversible solid-solid transition at 78.9°, and at 81.7° yields a nematic phase which transforms to the isotropic state at 104.4°. Earlier literature values[7] are 81.5° for the $K \rightarrow N$ transition, 108° for $N \rightarrow I$.

The crystal structure of this material, at room temperature, is of a sheet type. Each sheet is a bimolecular layer in which the molecular long axes are inclined at $\pm 18.5°$ to the sheet surface, but are otherwise parallel. Successive sheets, however, are oriented so that their director axes are mutually perpendicular. To achieve the classical all-parallel nematic arrangement, the molecules in adjacent sheets would have to rotate relative to one another about an axis other than the molecular long axis. The crystal structure suggests that such motions would most readily occur by rotation of entire sheets relative to one another. It is not known whether such movement takes place at the solid-solid or at the solid-nematic transition. An alternative model, involving only a displacive transition, would lead to a laminated structure for the mesophase having a negative order parameter.

EXPERIMENTAL

A *p*-[(*p*'-Ethoxybenzylidene)amino]benzonitrile

Crystal data. $C_{16}H_{14}N_2O$, mol · wt. 2503. Monoclinic, $a = 7.817(2)$, $b = 16.208(5)$, $c = 11.490(4)$ Å, $\beta = 112.76(5)°$, cell volume = 1342 Å, $D_{obs} = 1.22$ g cm^{-3} (by flotation), $Z = 4$, $D_{cal} = 1.238$ g cm^{-3}. Mo Kα radiation, $\lambda = 0.7107$ Å, $\mu = 1.2$ cm^{-1}. Space group $P2_1/c$.

Space group identification was made from the conditions governing diffraction: $h0l$ with $l = 2n$ only and $0k0$ with $k = 2n$ only as observed on 25° precession photographs taken with Mo Kα radiation. Cell dimensions were obtained by a least-squares fit to the observed diffractometer values of $\pm 2\theta$ for 20 strong general reflections.

Intensity measurements were made by standard automated diffractometry using a Picker four-circle instrument controlled by an XDS Sigma 2 computer. One quadrant of reciprocal space was surveyed with Mo Kα radiation to $2\theta = 50°$. Scattered intensity significantly above background $(I > 3\sigma(I))$] was measured by scintillation counting with pulse-height analysis at 1262 of the 2375 lattice points examined. The θ-2θ scan method was used with a scan range of 3° and a scan speed of 2° min^{-1} in 2θ. The intensities of two reference reflections, scanned after every 50 measurement cycles, showed a random fluctuation of 2.5% about their mean intensities. No absorption correction was applied and structure amplitudes and normalized structure amplitudes were derived in the usual ways.

Structure analysis and refinement Use of the program *MULTAN*[8] gave a series of phase sets of which the most favored yielded an *E*-map whose largest peaks corresponded to the molecular structure. However, this structure could not be refined below $R = 0.38$, and the true structure was found to involve a head-to-tail switch of the molecule which left most of the original peaks on the map as atomic sites. Refinement of the corrected structure proceeded smoothly by the block-diagonal least-squares method. Anisotropic thermal parameters were adopted for C, N, and O atoms. All hydrogen atoms were well defined in a three-dimensional difference electron-density map, and their positional and isotropic thermal parameters were included in the refinement as variables. A conventional weighting scheme was used,[9] and at convergence [$\Delta(p) < 0.08\sigma(p)$] the conventional weighted and unweighted residuals were 0.043 and 0.040, respectively. Scattering functions were taken from Ref. 17.

With the exception of *MULTAN*and *ORTEP*,[10] for which a CDC Cyber 172 computer was used, all computations were carried out using programs written in this laboratory for the XDS Sigma 2 computer.

B *p*-[(*p*'-Methoxybenzylidene)amino]phenyl acetate

Crystal data $C_{16}H_{15}NO_3$, mol. wt. 269.3. Orthorhombic, $a = 19.833(5)$, $b = 5.858(2)$, $c = 12.210(4)$ Å, cell volume = 1419 Å, $D_{obs} = 1.25$ g cm^{-3} (flotation), $Z = 4$, $D_{cal} = 1.270$ g cm^{-3}. Cu Kα radiation, $\lambda = 1.5418$ Å, $\mu = 7.0$ cm^{-1}. Space group $Pna2_1$.

Systematic absences of spectra on 25° precession photographs taken with Mo Kα radiation were: $0kl$ with $k + l$ odd and $h0l$ with h odd. These conditions can arise from space group $Pna2_1$ or *Pnam*. With four molecules in the unit cell, the latter space group requires either a molecular center of symmetry, which is impossible in the absence of disordering, or a molecular mirror plane which, though not impossible, is unlikely. The distribution of intensities also indicated a non-centrosymmetric space group, leading to the choice of $Pna2_1$.

Other experimental procedures were the same as for EOBABN, a single octant of reciprocal space being examined with Cu Kα radiation to $2\theta = 120°$. Intensity significantly above background was measured at 962 of 1125 reciprocal lattice points. Stability of the symmetry-equivalent reference intensities was to within 2% of their mean.

Structure determination and refinement The structure was solved routinely by application of the program *MULTAN*, and was refined in the same way as for EOBABN except that hydrogen atom parameters were not varied.

These atoms were held fixed in assumed idealized positions with C—H = 1.08 Å along the appropriate bisector. At convergence the weighted and unweighted residuals were 0.065 and 0.052 for the 962 reflections used. No attempt was made to establish absolute configuration.

RESULTS AND DISCUSSION

A Molecular Geometry and Conformation

Atomic coordinates and equivalent isotropic thermal parameters, together with their standard deviations, are given for EOBABN in Table I and for MOBAPA in Table II.[11] Diagrams of the two structures in the conformations adopted in the crystal and showing the numbering schemes adopted are shown in Figures 1 and 2. Bond lengths and angles are given in Table III.

A fair number of benzylideneanilines have been examined by the X-ray method,[12] and a consistent pattern of bond lengths and angles is found in the central region of these molecules. Previously observed values for the length of bond *a* (see key) lie between 1.398 and 1.460 Å, for bond *b* between 1.237 and 1.287 Å, and for bond *c* from 1.447 to 1.496 Å. Intramolecular steric repulsions cause the angles α, δ, and ϕ to be enlarged, and the angles β, γ, and ε to be reduced, from 120°. The observed bond lengths and angles in EOBABN and MOBAPA conform to this pattern. The value of 1.430(6) Å found in MOBAPA is the shortest length thus far observed for bond *c*, and is associated with the largest value thus far found for the angle δ, 126.0(5)°.

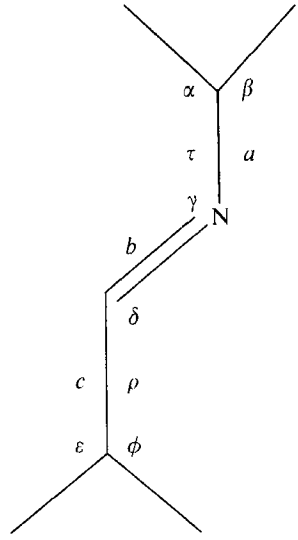

TABLE I

Atomic parameters defining the crystal structure of EOBABN

Atom	x	y	z	B
N(1)	627(4)	−250(1)	3501(2)	5.99
C(2)	915(4)	425(2)	3821(2)	4.75
C(3)	1270(3)	1273(2)	4209(2)	3.98
C(4)	2067(4)	1476(2)	5473(3)	4.64
C(5)	2342(4)	2288(2)	5832(2)	4.54
C(6)	1831(3)	2918(2)	4939(2)	3.88
C(7)	1043(4)	2703(2)	3670(3)	4.64
C(8)	773(4)	1890(2)	3309(3)	4.78
N(9)	2098(3)	3736(1)	5396(2)	4.22
C(10)	2378(4)	4305(2)	4734(2)	4.14
C(11)	2645(3)	5165(1)	5136(2)	3.75
C(12)	2635(4)	5421(2)	6285(2)	4.40
C(13)	2946(4)	6225(2)	6655(2)	4.61
C(14)	3264(3)	6809(2)	5873(2)	3.86
C(15)	3266(4)	6571(2)	4723(2)	4.45
C(16)	2970(4)	5750(2)	4371(2)	4.47
O(17)	3556(3)	7597(1)	6331(2)	4.84
C(18)	3814(4)	8236(2)	5548(3)	4.83
C(19)	4171(4)	9023(2)	6288(3)	5.84
H(4)	239(4)	108(1)	606(2)	4.7(6)
H(5)	291(3)	242(2)	673(2)	5.6(6)
H(7)	69(4)	315(2)	308(3)	7.1(7)
H(8)	20(4)	174(2)	244(2)	6.0(6)
H(10)	250(3)	417(1)	391(2)	4.5(5)
H(12)	238(3)	504(1)	680(2)	4.1(5)
H(13)	288(3)	638(1)	746(2)	5.0(6)
H(15)	348(3)	695(1)	420(2)	4.4(5)
H(16)	299(3)	557(1)	355(2)	4.9(6)
H(18a)	260(3)	828(1)	479(2)	5.4(6)
H(18b)	489(4)	808(2)	529(3)	6.9(7)
H(19a)	445(4)	945(2)	579(3)	7.0(7)
H(19b)	303(5)	916(2)	649(3)	9.7(9)
H(19c)	524(4)	895(2)	711(3)	7.8(8)

Positional parameters are given as fractions of the unit cell edges, C, N, and O $\times 10^4$, H $\times 10^3$. Thermal parameters are given as equivalent isotropic B values (Å^2) for C, N, and O and as actual B values for H. Standard deviations are given in parentheses, where applicable, and apply to the least significant digits given.

TABLE II

Atomic parameters defining the crystal structure of MOBAPA

Atom	x	y	z	B
C(1)	509(3)	11141(11)	4134(5)	6.85
C(2)	713(2)	9214(10)	3419(4)	5.01
O(1)	1032(2)	7570(10)	3665(4)	9.76
O(2)	459(2)	9436(6)	2419(3)	4.77
C(3)	620(2)	7809(8)	1621(5)	4.30
C(4)	234(2)	5807(9)	1580(5)	4.89
C(5)	364(2)	4275(9)	716(5)	4.95
C(6)	863(2)	4697(9)	−43(4)	4.12
C(7)	1234(2)	6718(9)	29(5)	4.64
C(8)	1103(2)	8226(9)	853(4)	4.62
N(9)	969(2)	3054(8)	−863(3)	4.65
C(10)	1569(2)	2666(9)	−1214(5)	4.89
C(11)	1755(2)	998(9)	−2014(4)	4.16
C(12)	1280(2)	−377(10)	−2534(5)	4.84
C(13)	1474(2)	−2091(10)	−3265(5)	4.96
C(14)	2145(2)	−2408(10)	−3464(5)	4.93
C(15)	2627(3)	−1098(9)	−2975(5)	5.25
C(16)	2430(3)	610(10)	−2240(5)	5.23
O(17)	2390(2)	−4114(7)	−4167(3)	6.49
C(18)	1927(3)	−5714(10)	−4602(5)	5.77
H(1a)	62	1273	373	7.8
H(1b)	77	1101	492	7.8
H(4)	−15	545	219	5.9
H(5)	67	274	65	6.0
H(7)	162	708	−56	5.6
H(8)	139	979	90	5.6
H(10)	197	370	−87	5.9
H(12)	75	−11	−237	5.8
H(13)	110	−314	−366	6.0
H(15)	315	−138	−315	6.3
H(16)	281	164	−184	6.2
H(18a)	219	−681	−520	6.8
H(18b)	153	−483	−501	6.8
H(18c)	174	−677	−396	6.8

Positional parameters are given as fractions of the unit cell edges, C, N, and O $\times 10^4$, H $\times 10^3$. Equivalent isotropic B values are given for C, N, and O, together with those assumed for H. Standard deviations are given in parentheses, where appropriate, and are applicable to the least significant digits given.

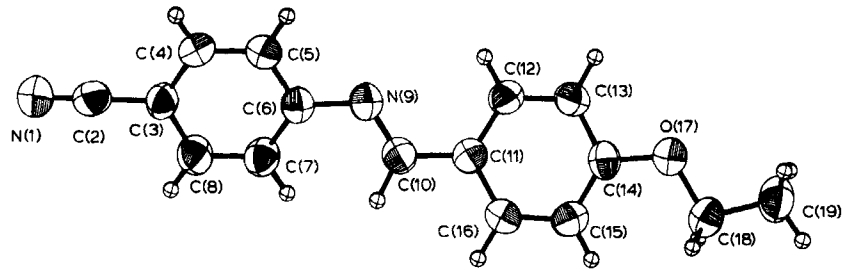

FIGURE 1 *ORTEP* drawing of EOBABN in the conformation found in the crystal, and showing the numbering scheme adopted. Thermal ellipsoids for C, N, and O are drawn to the 50% probability level. Hydrogen atoms are denoted by spheres of arbitary radius and are numbered to correspond to the atom of attachment.

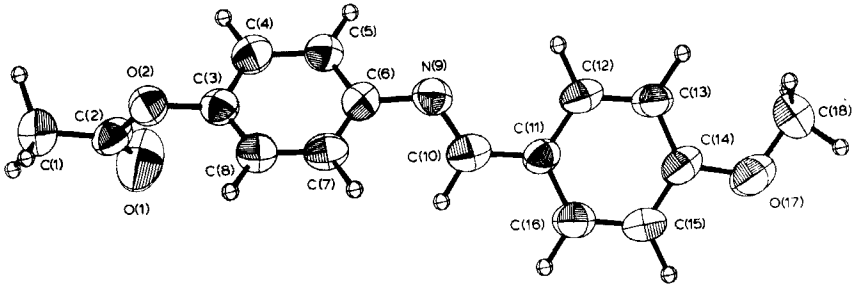

FIGURE 2 *ORTEP* drawing of MOBAPA in the conformation found in the crystal, and showing the numbering scheme adopted. Thermal ellipsoids for C, N, and O are drawn to the 50% probability level. Hydrogen atoms are denoted by spheres of arbitrary radius and are numbered to correspond to the atom of attachment.

TABLE III

Bond distances and angles with their standard deviations for EOBABN and MOBAPA

Distances (Å)	EOBABN	MOBAPA
N(1)—C(2)	1.148(3)	
C(1)—C(2)		1.483(8)
C(2)—O(1)		1.191(7)
C(2)—O(2)		1.326(6)
C(3)—O(2)		1.400(6)
C(2)—C(3)	1.438(3)	
C(3)—C(4)	1.381(3)	1.401(6)
C(3)—C(8)	1.382(3)	1.362(7)
C(4)—C(5)	1.371(3)	1.409(7)
C(5)—C(6)	1.392(3)	1.377(7)
C(6)—C(7)	1.390(3)	1.398(7)

TABLE III (*continued*)

Distances (Å)	EOBABN	MOBAPA
C(6)—N(9)	1.412(3)	1.405(6)
C(7)—C(8)	1.373(3)	1.364(7)
N(9)—C(10)	1.269(3)	1.286(6)
C(10)—C(11)	1.458(3)	1.430(7)
C(11)—C(12)	1.387(3)	1.393(7)
C(11)—C(16)	1.381(2)	1.386(6)
C(12)—C(13)	1.363(2)	1.398(8)
C(13)—C(14)	1.391(2)	1.365(6)
C(14)—C(15)	1.377(3)	1.363(7)
C(14)—O(17)	1.367(2)	1.404(6)
C(15)—C(16)	1.385(2)	1.399(7)
O(17)—C(18)	1.436(2)	1.415(6)
C(18)—C(19)	1.497(3)	

Angles (deg.)	EOBABN	MOBAPA
N(1)—C(2)—C(3)	179.4(10)	
C(1)—C(2)—O(1)		127.7(5)
C(1)—C(2)—O(2)		111.3(5)
O(1)—C(2)—O(2)		120.8(5)
C(2)—O(2)—C(3)		119.2(4)
O(2)—C(3)—C(4)		118.0(4)
C(2)—C(3)—C(4)	120.6(2)	
O(2)—C(3)—C(8)		121.2(4)
C(2)—C(3)—C(8)	119.7(2)	
C(4)—C(3)—C(8)	119.8(2)	120.7(5)
C(3)—C(4)—C(5)	120.0(2)	117.4(5)
C(4)—C(5)—C(6)	121.0(2)	121.4(5)
C(5)—C(6)—C(7)	118.3(2)	119.2(5)
C(5)—C(6)—N(9)	117.1(2)	117.7(4)
C(7)—C(6)—N(9)	124.6(2)	123.1(5)
C(6)—C(7)—C(8)	120.7(2)	119.6(5)
C(7)—C(8)—C(3)	120.2(3)	121.7(5)
C(6)—N(9)—C(10)	119.7(2)	119.8(4)
N(9)—C(10)—C(11)	122.9(2)	126.0(5)
C(10)—C(11)—C(12)	122.3(2)	122.2(4)
C(10)—C(11)—C(16)	119.5(2)	119.8(5)
C(12)—C(11)—C(16)	118.1(2)	117.9(5)
C(11)—C(12)—C(13)	121.1(2)	121.4(4)
C(12)—C(13)—C(14)	120.2(2)	118.7(5)
C(13)—C(14)—C(15)	119.8(2)	121.9(5)
C(14)—C(15)—C(16)	119.2(2)	119.2(5)
C(15)—C(16)—C(11)	121.6(3)	121.0(5)
C(13)—C(14)—O(17)	115.6(2)	122.9(5)
C(15)—C(14)—O(17)	124.6(2)	115.2(4)
C(14)—O(17)—C(18)	118.5(2)	118.4(4)
O(17)—C(18)—C(19)	107.4(2)	

Other bond distances and angles have expected values. The aniline ring of EOBABN shows marked quinoid character, having experimentally exact C_s symmetry about the C(3)—C(6) axis and with C(4)—C(5) and C(7)—C(8) equal and significantly shorter than the other ring bonds.

In the benzylidene ring of EOBABN the pattern of bond distances is similar to that found in *p*-[(*p'*-methoxybenzylidene) amino]phenol,[13] with marked shortening of the C(12)—C(13) bond trans to C(14)—O(17) and on the opposite side of the molecule from the alkyl substituent, indicating a semi-quinoidal character. Both EOBABN and the phenol have the —N=CH— and —O—CH_2— bonds trans with respect to the 1,4-axis of the ring. In MOBAPA these two bonds are *cis* to one another and a quite different pattern of bond lengths is found. Colapietro and Domenicani[14] have interpreted the ring geometry of benzoic acids in terms of distortions of the C_s symmetry of the phenyl ring caused by introduction of the alkoxy substitutents. Similar effects presumably operate in these 1,4-disubstituted systems, with the observed geometry depending on the particular distortions of symmetry present.

The overall molecular conformations of benzylideneanilines are conventionally described with respect to three planar groups of atoms: (1) the plane of the aniline ring; (2) the plane of the central four-atom group C(6)—N(9)—C(10)—C(11); and (3) the plane of the benzylidene ring. Information on these planes is given in Table IV, which also lists (4), the plane of the acetate group in MOBAPA.

The torsion angles τ and ρ, the (1)–(2) and (2)–(3) interplanar angles, are −29.0° and 1.2°, respectively, in EOBABN, and 35.6° and 5.4° in MOBAPA (29.0° and −1.2°; −35.6° and −5.4°, for the enantiomeric members also present in the crystals). These values lie within previously observed limits

TABLE IV

Least-squares mean planes for selected groups of atoms as defined in the text

Plane	Molecule	*a*	*b*	*c*	*d*	Δ_{ave}	Δ_{max}
(1)	EOBABN	−0.99895	0.03266	0.03212	1.08272	5	3
	MOBAPA	0.67247	−0.46580	0.57517	−0.16801	10	5
(2)	EOBABN	0.88477	−0.15841	0.43828	0.87190	4	4
	MOBAPA	0.12107	−0.69189	0.71178	−1.74538	14	12
(3)	EOBABN	0.88325	−0.17839	0.43365	0.67602	5	3
	MOBAPA	0.04796	−0.65322	0.75564	−2.07179	2	1
(4)	MOBAPA	−0.83032	−0.48694	0.27103	−2.65295	18	9

Coefficients are given for the equations in the form: $aX + bY + cZ = d$ where X, Y, and Z are in Å with respect to a Cartesian axial system. For EOBABN $X = x + z.\cos\beta$, $Y = y$, and $Z = z.\sin\beta$. Average and maximum displacements from the planes of atoms included in the calculation are given as Å × 10^3.

for benzylideneanilines. The preferred conformations have been analyzed by Bürgi and Dunitz,[15] who have considered electronic *vs* steric factors, by Bernstein and Hagler,[16] who have considered the effect of crystal environment, and by Nakai *et al.*,[12] who have discussed the role played by substituents.

In EOBABN, N(1), C(2), and N(9) are displaced from plane (1) by 0.088, 0.052, and 0.057 Å, respectively. N(9), C(10), O(17), C(18), and C(19) lie, respectively, 0.053, 0.037, 0.006, −0.053, and 0.016 Å from plane (2).

In MOBAPA, O(2) and N(9) are displaced from plane (1) by −0.095 and 0.021 Å, respectively. N(9), C(10), O(17), and C(18) lie, respectively, 0.199, 0.080, 0.028, and 0.196 Å from plane (2). The plane of the acetate group makes an angle of 100.1° with plane (1), 64.6° with plane (2), and 61.1° with plane (3).

B Molecular packing in the crystal

I. EOBABN Diagrams of the molecular arrangement in the crystal are given in Figures 3, 4, and 5. The molecules are aligned, in a head-to-tail fashion, in rows parallel to the crystal *b*-axis. Molecules in adjacent rows in the *a*-direction are related by the crystallographic centers of symmetry (Figure 3), and in the *c*-direction by the two-fold screw axes (Figure 4). The molecular long axis, defined as the axis N(1)—C(19), makes angles of ±84.3° with the crystal *a*-axis, ±12.5° with *b*, and ±82.0° with *c*.

Figure 5 shows the molecular packing in *b*-axis projection, a view down the potential director axis of the mesophase. A given molecule makes lateral contacts with ten neighboring molecules, and end-to-end contact with four others.

The molecular orientation in the crystal may be expressed in terms of the familiar nematic order parameter,

$$\langle P_2 \rangle = \tfrac{1}{2}(3\langle \cos^2 \theta \rangle - 1),$$

by choosing the crystal *b*-axis as the director axis. The angle made by the molecular long axis with *b* is ±12.5°, leading to a value for $\langle P_2 \rangle$ of 0.93. One cannot, of course, extrapolate directly from the crystal order parameter to that for the mesophase, but it is reasonable to suppose that the crystal value represents a maximum value for the order parameter for this material. The crystal order parameter is also sufficiently high to make it probable that the transition to the nematic phase is accomplished through simple relaxations of the intermolecular attractive forces with increasing thermal energy in such a way that translational motion of the molecules becomes possible, perhaps accompanied by rotation about the molecular long axis, while the

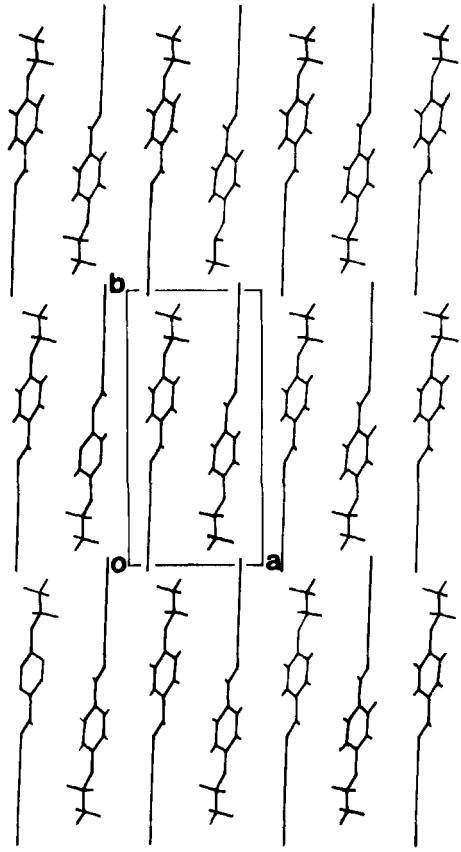

FIGURE 3 Sheet of molecules in the crystal of EOBABN, projected onto the *ab*-plane.

overall molecular matrix acts to constrain rotations about other molecular axes. The transition would then be of the displacive type.

We have shown in previous crystal structure analyses that a nearly parallel alignment of molecules in the crystal is not, of itself, a sufficient condition for mesophase formation. It is also necessary that the energy of the crystal packing is such that the forces holding molecules together can be overcome at a temperature at which the molecules have not yet acquired sufficient thermal energy to rotate about axes other than the long axis.

Thus, we have earlier described the crystal structures of *p*-methoxy- and *p*-ethoxy-benzoic acids,[18] in which mesophase formation is inhibited at atmospheric pressure by overly tight molecular packing, even though the spatial requirements of molecular parallelism have already been met.[19]

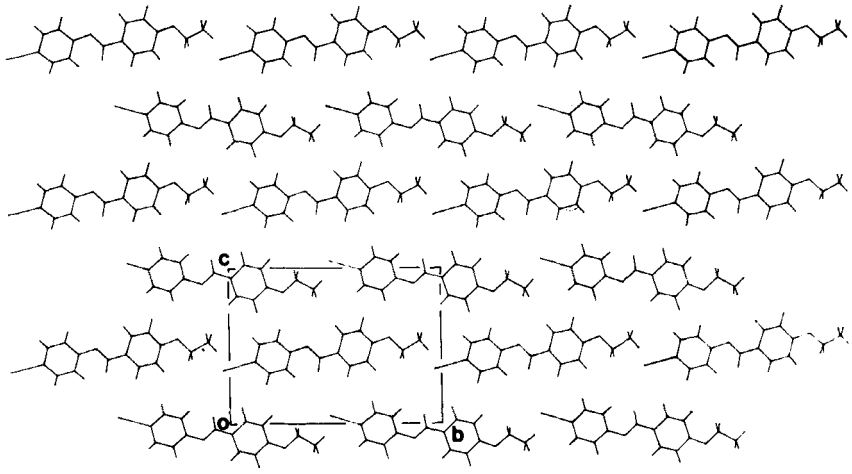

FIGURE 4 Sheet of molecules in the crystal of EOBABN, projected onto the *bc*-plane.

We have also argued in similar terms concerning the failure of *p*-hydroxy-*trans*-cinnamic acid to form a mesophase, an otherwise spatially suitable crystal structure precursor being stabilized beyond an appropriate transition temperature by hydrogen bonding.[20]

It is therefore an important aspect of the molecular packing in EOBABN that there are no particularly strong interactions between molecules in the

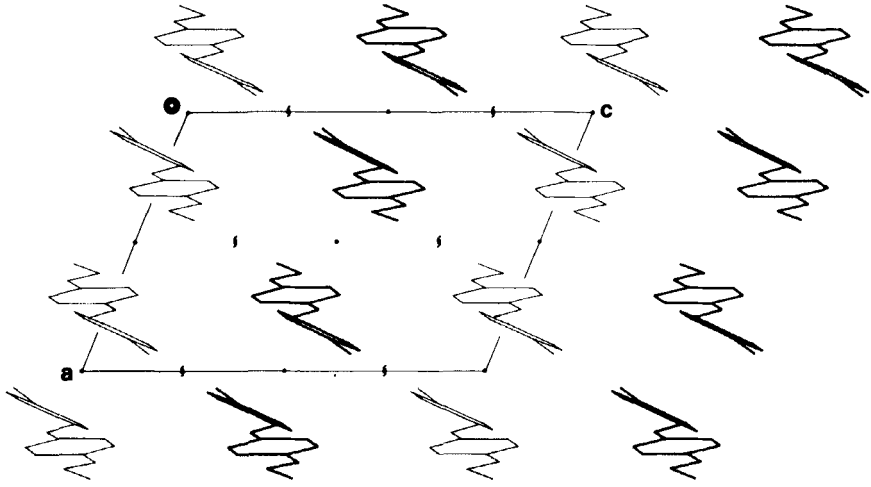

FIGURE 5 Molecular packing in the EOBABN crystal, viewed in *b*-axis projection. Relative heights of molecules in *b* are indicated by the different line thicknesses.

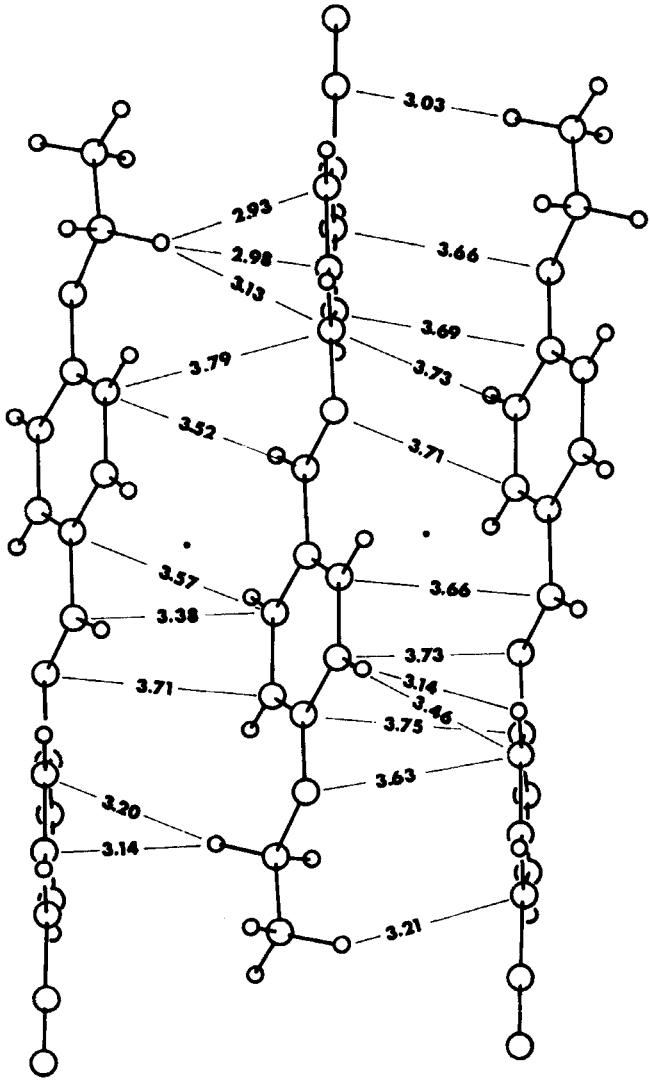

FIGURE 6 Contacts (Å) between molecules related by a center of symmetry in the crystal of EOBABN.

crystal, a fact attested to also by the quite low K → N transition temperature of 105°. There are no strong dipole-dipole interactions involving the polar groups in the molecule, such as have been identified in the crystal structures of certain other mesogens.[21] Whereas such interactions may play a role in stabilizing mesophase organization, particularly in the case of smectics, we believe that such forces are as likely to act in a destabilizing sense, by requiring higher thermal energies for lattice breakdown in the solid. Such higher energies would then tend to favor acquisition of additional degrees of freedom at the transition to the melt.

Only two limiting van der Waals contracts are found in the crystal of EOBABN between atoms other than hydrogen. These are between atoms in centrosymmetrically related molecules: C(10) ··· C(16), 3.375 Å and C(7) ··· C(13), 3.462 Å. Also limiting are the contacts between the same pairs of molecules involving the methylene hydrogen atom H(18b) and C(4) and C(5). These and other contacts between the centrosymmetrically related molecules are shown in Figure 6. With the exception of the close contacts mentioned, other intermolecular approaches are comfortably in excess of the sums of the van der Waals radii of the atoms involved. A complete list of intermolecular approach distances <4.0 Å is available on request to the authors.

II. MOBAPA The crystal structure of this compound offers a striking contrast to that of EOBABN, and to the type of crystal structure normally found for a nematogen. The packing in the crystal may be described in terms of a sheet structure. Each sheet is a bimolecular layer, and the director axes of successive sheets lie in parallel planes normal to *a*, but the axes are mutually perpendicular from layer to layer. The packing may be understood from the stereoscopic views given in Figure 7.

The basic structural unit is taken as the set of molecules related by translations in *b* and *c*, as seen in Figure 7(a). The molecular long axis is taken as O(2)–O(17). The long axes of molecules in this set are parallel, and they make an angle of 18.7° with the *bc*-plane. The action of the space-group *n*-glide operation adds to this set a second set of molecules to complete the sheet element, as shown in Figure 7(b). The long axes of molecules of the second set lie in parallel planes normal to the *bc*-plane, but are inclined to that plane at $-18.7°$. A crystal director axis may be chosen to give a minimum deviation from the long axial directions. That axis will lie in the plane of the sheet element, parallel to the *bc*-plane, and making an angle with *c* of 44.6°.

The operation of the space-group 2_1-axes, which lie parallel to *c*, generates an identical sheet element, again with a director axis lying parallel to the *bc*-plane but making an angle of $-44.6°$ with *c*. The director axes of adjacent

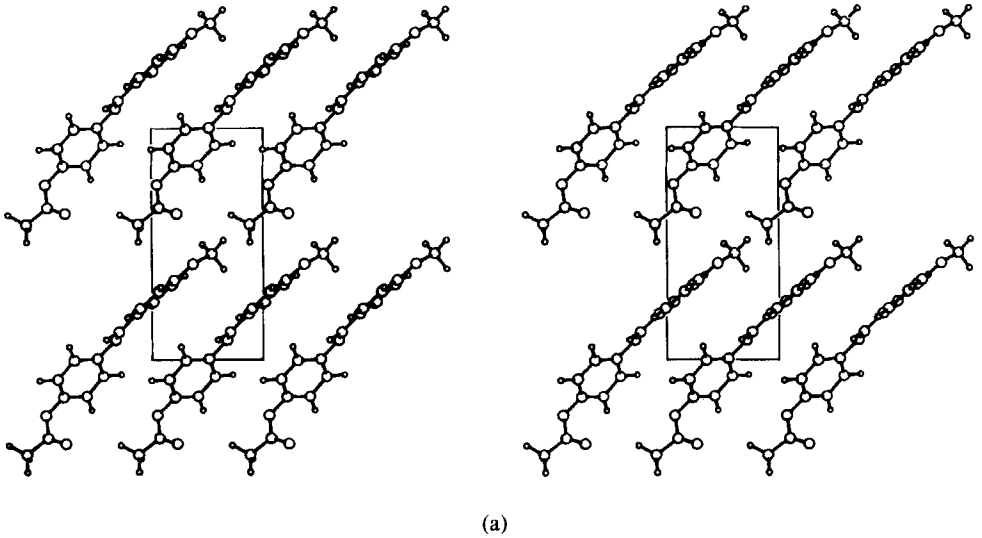

(a)

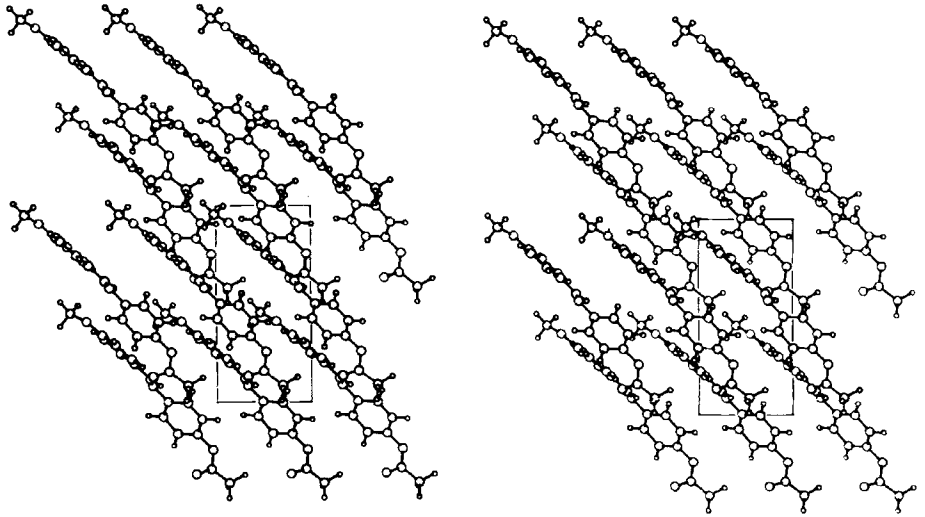

(b)

FIGURE 7 (a) Stereoscopic view of molecules of MOBAPA related by translations in *b* (horizontal) and *c* (vertical). (b) Stereoscopic view of a bimolecular sheet of molecules of MOBAPA. To the set in Figure 7(a) has been added a second set related to the first by the *n*-glide operation.

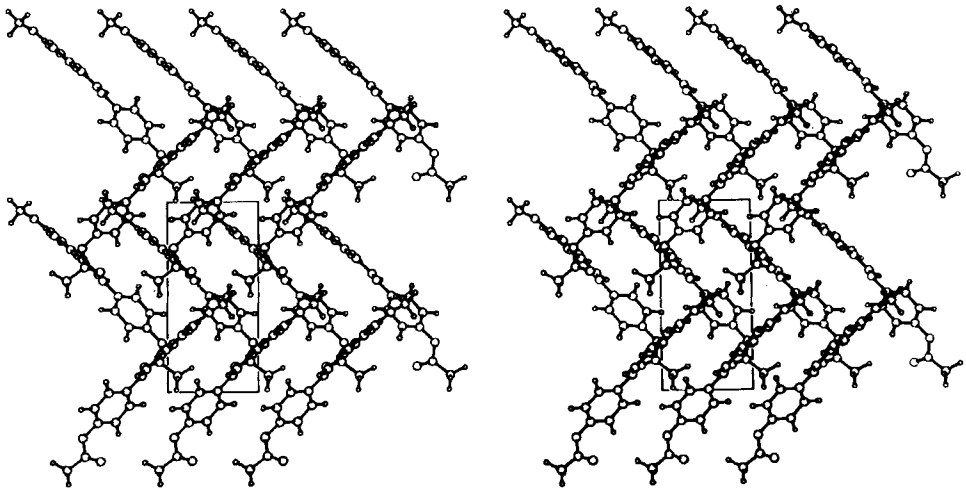

(c)

FIGURE 7 (c) Stereoscopic view of the relation between adjacent sheets of molecules of MOBAPA. One set of molecules from each of two sheets is shown.

sheets thus lie in parallel planes, but are virtually at right angles to one another. A single set of molecules from each of two screw-axis related sheets is shown in Figure 7(c).

A view of the molecular packing in *b*-axis projection is shown in Figure 8.

An overall director axis for the crystal, chosen so as to minimize divergences between it and the directions of the molecular long axes, lies parallel to the *bc*-plane and bisects the angle between the sheet director axes. This choice

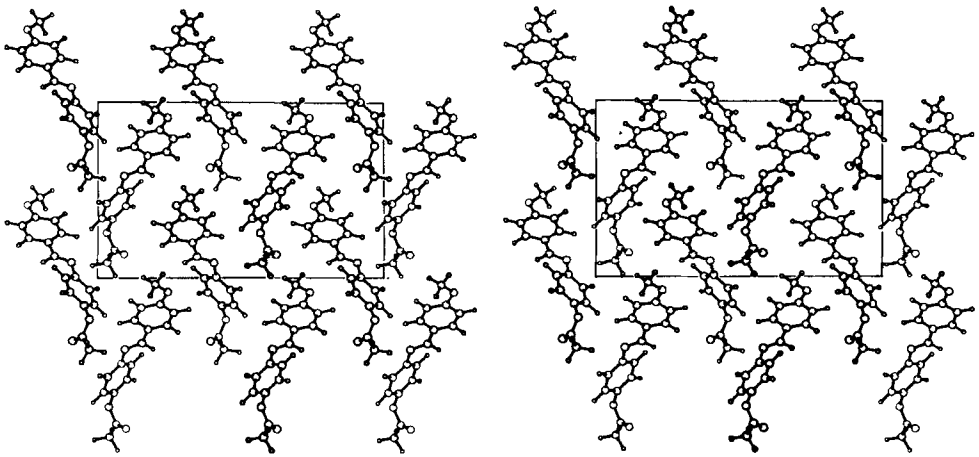

FIGURE 8 Stereoscopic view of molecular packing in MOBAPA, seen in *b*-axis projection.

gives $\langle\theta\rangle = 44.6°$ and $\langle P_2\rangle = 0.26$. That value lies below both the theoretical and the experimentally determined stability limits for a classical nematic phase.[22] The transformation to a classical nematic phase would thus require rotations of the molecules relative to one another at the transition point, about axes other than the molecular long axis, to achieve an acceptable degree of parallel alignment. Such a process involves rotations which are formally forbidden in the ideal nematic phase, as they diminish rather than enhance order. To achieve a classical nematic phase from this crystal structure would therefore require a reconstitutive transition.

It is, of course, possible that such a process takes place at the solid-solid transition rather than at the solid-nematic transition, and the existence of a reconstitutive solid-nematic transition cannot be assumed in the absence of information on the structure of the high-temperature solid. Given the sheetlike character of the low temperature solid, it seems probable that the transformation to the all-parallel alignment likely in the nematic phase proceeds by rotation of the sheet elements about the crystal a-axis at one or the other transition.

There is an intriguing alternative for the molecular arrangement in the nematic phase if we assume that the solid-solid transition involves no radical reorganization of the molecules and that the solid-nematic transition is displacive. The molecules would then have translational motion only within the individual sheets, as the normal restrictions on rotations about minor axes would be present and the orthogonal juxtaposition of the long axes of molecules in adjacent layers would tend to preserve a sheet character in the mesophase.

Such a phase, lacking a translational degree of freedom, would normally have the character of a smectic phase. It differs from a classical smectic, however, by having the long axes of the molecules more nearly parallel than normal to the layer boundary. The director axis for such a phase might then be chosen quite differently, as normal to the sheets rather than parallel to them. For the crystal phase this yields $\langle\theta\rangle = 71.3°$ and gives $\langle P_2\rangle = -0.35$, a negative order parameter. Structures involving negative order parameters are considered to be thermodynamically less stable than those on the upper branch of the order parameter curve,[23] and if there is rotation of molecules about their long axis it is difficult to imagine a phase of this kind remaining stable with respect to the normal nematic alignment. In the absence of such rotation, however, cases can be envisioned where a crossed-sheet phase resulting from a displacive solid-nematic transition might be stable.

Acknowledgement

This work was supported, in part, by a grant (DMR 78-19884) from the National Science Foundation.

References

1. A. Saupe, *Liquid Crystals and Plastic Crystals*, G. W. Gray, P. A. Winsor, eds., Halstead Press, Chichester, Vol. 1, 1974, pp. 18 ff.
2. V. Zwetkoff, *Acta Physicochim. URSS*, **16**, 132 (1942); W. Maier and A. Saupe, *Z. Naturforsch.*, **A13**, 564 (1958); **14**, 882 (1959); **15**, 287 (1960); A. Saupe, *ibid.*, **15**, 810 and 815 (1960).
3. The terms *displacive* and *reconstitutive* have been applied by M. J. Buerger with somewhat different meaning to transitions in inorganic solids. In their usage here they correspond to the terms *homeomorphic* and *morphotropic* used by J. D. Bernal and D. Crowfoot, *Trans. Faraday Soc.*, **29**, 1032 (1933).
4. M. Cotrait, D. Sy, and M. Ptak, *Acta Crystallogr.*, **B31**, 1869 (1975).
5. R. F. Bryan, *Proc. Organic Crystal Chemistry Symp., Poznan-Dymaczewo*, p. 105 (179).
6. E. Frolich, Dissertation, Halle (1910).
7. P. Hansen, Dissertation, Halle (1907).
8. G. Germain, P. Main, and M. M. Woolfson, *Acta Crystallogr.*, **A27**, 368 (1971).
9. P. W. R. Corfield, R. J. Doedens, and J. A. Ibers, *Inorganic Chem.*, **6**, 197 (1967).
10. C. K. Johnson, OR-TEP II, *A Fortran Thermal Ellipsoid Plot Program for Crystal Structure Illustrations*, ORNL-5138, Oak Ridge National Laboratory, Oak Ridge (1976).
11. Tables of anisotropic thermal parameters and lists of observed and calculated structure amplitudes for the two compounds are available from the authors on request.
12. Data from the following sources are collected in Ref. 13: H. B. Bürgi and J. D. Dunitz, *Chem. Commun.*, 472 (1969); J. Bernstein, *J. Chem. Soc. Perkin Trans. II*, 951 and 946 (1972); B. T. Blaylock, M. S. Thesis, University of Virginia, (1973); D. P. Lesser, A. de Vries, J. W. Reed, and G. H. Brown, *Acta Crystallogr.*, **B31**, 653 (1975); see also H. Nakai, M. Shiro, K. Ezumi, S. Sakata, and T. Kubota, *ibid.*, **B32**, 1827 (1976).
13. R. F. Bryan, P. Forcier, and R. W. Miller, *J. Chem. Soc. Perkin Trans. II*, 368 (1978).
14. M. Colapietro and A. Domenicano, *Acta Crystallogr.*, **B34**, 3277 (1978).
15. H. B. Bürgi and J. D. Dunitz, *Helv. Chim. Acta*, **54**, 1255 (1971).
16. J. Bernstein and A. T. Hagler, *Abstr. Amer. Crystallogr. Assocn.*, **6**, 16 (1978).
17. D. T. Cromer and J. T. Waber, *International Tables for X-Ray Crystallography*, Kynoch Press, Birmingham, (1974), Vol. IV; R. F. Stewart, E. R. Davidson, and W. T. Simpson, *J. Chem. Phys.*, **42**, 3175 (1965).
18. R. F. Bryan, *J. Chem. Soc. (B)*, 1311 (1967); R. F. Bryan and J. J. Jenkins, *J. Chem. Soc. Perkin Trans. II*, 1171 (1975).
19. *p*-Ethoxybenzoic acid forms both a smectic and a nematic phase at high pressures; see S. Chandrasekhar, A. S. Reshamwala, B. K. Sadashiva, R. Shashidhar, and V. Surendranath, *Pranana, Suppl.*, **1**, p. 117 (1973).
20. R. F. Bryan and D. P. Freyberg, *J. Chem. Soc. Perkin Trans. II*, 1835 (1975).
21. See, for example, M. Cotrait, and M. Pesquer, *Acta Crystallogr.*, **B33**, 2826 (1977).
22. G. W. Smith, *Advances in Liquid Crystals*, Academic Press, New York, Vol. 1, p. 189 (1975).
23. E. B. Priestly, P. J. Wojtowicz, and P. Sheng, eds., *Introduction to Liquid Crystals*, Plenum Press, New York, (1974).